Proceedings of the Canadian Society for Mechanical Engineering International Congress
32nd Annual Conference of the Computational Fluid Dynamics Society of Canada
Canadian Society of Rheology Symposium
CSME/CFDSC/CSR 2025
May 25–28, 2025, Montréal, Québec, Canada

GRASP-01 A Low-Cost 7 Degree of Freedom Humanoid Robotic Arm

Kenneth Martinez[1], Riley Workman[1], Md Shafakat Masud[1,2], Lang H.[1]

[1]Department of Mechatronics and Manufacturing Engineering, Ontario Tech University, Oshawa, Canada
[2]Department of Nuclear Science and Engineering, Military Institute of Science and Technology, Dhaka, Bangladesh

***Abstract*—**Despite significant technological advances in humanoid robotics, widespread adoption remains limited due to high manufacturing costs that restrict accessibility. This paper presents GRASP-01, a low-cost 7 Degree of Freedom (DOF) humanoid robotic arm designed to address these economic barriers while maintaining functional integrity through Fused Deposition Modeling (FDM) materials and optimized geometric design. The prototype achieves a total mass of 5.6 kg. It incorporates integrated servo motors with position control, a direct-drive configuration, and CAN bus communication. It was tested with a conservative initial payload capacity of 2 kg to maintain the system's stability during the initial stage of development; however, there is a potential for an increase in payload capacity through the enhancement of the mechanical system with further development and a maximum reach of 0.75 meters at full extension. Furthermore, it establishes a cost-effective humanoid robot arm development framework suitable for research and educational applications.

***Keywords-component*—humanoid robot, FDM, 7 DOF, URDF, Robot Arm**

I. INTRODUCTION

Humanoid robotics has rapidly advanced in recent years, driven by the need for adaptable, intelligent, and cost-effective robotic systems capable of interacting safely with humans and performing complex tasks. Traditionally, humanoid robotic arms have been developed with high-precision actuation, rigid structures, and closed-source control architectures, making them expensive and inaccessible for broader applications in research and industry. While industrial robotic systems, such as those used in manufacturing, excel in precision and repeatability, they often lack affordability and adaptability for environments outside structured industrial settings [1]. While companies like Tesla and Unitree Robotics are priced between 16,000 and 20,000 US Dollars, such costs remain prohibitive for broader accessibility [2]. A critical challenge in humanoid robotics is balancing cost, performance, and structural robustness. Recent efforts have explored fused deposition modelling (FDM) materials, diverse types of actuators, and intelligent sensing systems to create more affordable robotic arms while maintaining high functionality.

This paper presents GRASP-01, a low-cost humanoid robotic arm that explores the feasibility of utilizing FDM materials and other low-cost alternatives in constructing HR components to address these cost barriers while maintaining functional integrity. Our approach focuses on optimizing the design geometry of joint covers, internal components, and structural elements to ensure low stress distribution and high structural strength despite using more economical materials. The GRASP-01 platform implements these design principles in a 7 DOF configuration, enabling comprehensive functional testing in a kinematic arrangement comparable to industrial humanoid robotic systems, as shown in Fig. 1.

Figure. 1. The GRASP-01 humanoid robotic arm has optimized geometrics designs, achieving a total system mass of 5.6 kg. The modular architecture enables future geometric refinements for enhanced performance characteristics

Critical parameters must be considered when optimizing robotic arm components manufactured through FDM. As demonstrated in [3], process parameters such as layer height, printing speed, extrusion temperature, and material selection significantly influence printed components' mechanical properties and structural integrity. The precise configuration of these parameters is fundamental for achieving an optimal balance between mass reduction and mechanical performance in robotic applications. In [4], successful implementation was demonstrated using polyamide and PLA materials with trellis-like internal structures, achieving enhanced structural integrity while facilitating heat dissipation through improved air circulation in their robotic arm design. Building upon this structural approach in [5], FDM is applied by optimizing print parameters for precision gear components, utilizing fine layer heights and specialized infill patterns to create a lightweight yet robust planetary gearbox. This combined knowledge demonstrates how careful consideration of FDM parameters and structural design can enable the development of cost-effective and functional robotic components, particularly for joint mechanisms requiring high precision and durability.

Objectives:

- Design considerations when using FDM materials
- Finite Element Analysis (FEA) for optimal design
- 7 DOF configuration with direct drive servo motors
- Cost analysis with FDM materials

II. RELATED WORK

The development of robotic manipulators has been at the forefront of modern research, particularly in the quest for cost-effective, compliant, and adaptive systems that can function efficiently in both structured industrial settings and unstructured human-centric environments. Quasi-Direct Drive (QDD) actuation has emerged as a pivotal innovation in achieving compliant and force-controlled manipulation in robotic arms. Gealy et al. introduced the "Blue" robotic arm, a 7-DOF human-scale manipulator designed to operate in unconstrained environments with an emphasis on affordability and safety. By employing QDD actuators with timing belt transmissions, the arm demonstrated high back-drivability and compliance, achieving a position-control bandwidth of 7.5 Hz and repeatability within 4 mm. The modular structure and use of lightweight materials reduced manufacturing costs to under 5,000 US Dollars, making it a promising candidate for broader deployment in household and industrial tasks. However, the arm's payload capacity of 2 kg and torque hysteresis issues highlighted areas requiring further optimization, particularly for tasks involving higher loads or prolonged operations [6]. Similarly, Zhao et al. expanded on the potential of QDD actuation in collaborative robotics, emphasizing its capability to enhance compliance and proprioception. Their work demonstrated robust trajectory tracking and safe interaction with humans, though the designs faced limitations in thermal performance and scalability under extended operational conditions [7]. Material optimization solves two key design problems by reducing weight without sacrificing structural strength. Alshihabi et al. proved that modal analysis and topology optimization can build lightweight robotic arm lattice structures that eliminate vibrations. These optimization techniques improved robotic systems' performance and stability, yet their high processing demands created issues for real-time use [3].

In related research, Chowdhury et al. demonstrated that thermoplastic polyurethane (TPU) auxetic structures offer better flexibility and impact resistance for robot arm exteriors. The approach demonstrated apparent success in minimizing strain during robot-human contact. However, according to them, there is a need for further research to understand how these printed materials perform under dynamic stress [8]. Costa et al. showed that open-source designs offer value by building a Thor robotic arm using ABS materials to create a 6-DOF manipulator. The economic benefits and flexibility of 3D printing brought challenges due to its limited load capacity and use of everyday consumer materials for demanding applications [9].

Researchers now emphasize creating systems that can function through multiple components or use additional parts to maintain performance. Nuhel et al. created a modular robotic manipulator with three degrees of freedom that integrates into a seven-degree-of-freedom robotic arm. The design used URDF-based custom controllers to deliver highly accurate path planning and movement execution. The design's modular construction enabled better flexibility in use and provided backup systems to safeguard operations. However, the system requires additional autonomous planning and control features because users currently define all the trajectories [10]. Hrdlička built a 3D-printed planetary gearbox that helped reduce robotic arm joint costs and extended their service life. The gearbox used PLA and PETG materials to transmit high torque at much lower costs than traditional gearboxes, but their material properties limited their durability and extended use [5].

Mick et al. introduced the Reachy robotic arm, a 7-DOF human-like manipulator designed with compliance and adaptability in mind. Utilizing 3D-printed components and open-source designs, Reachy was developed to facilitate human-robot interaction through intuitive control methods such as gaze-based object manipulation and teleoperation. Its modular structure and affordability make it an attractive platform for research and applications in rehabilitation and assistive robotics. However, its reliance on consumer-grade 3D-printed materials raises concerns about long-term durability, and its payload capacity limits its use in more demanding industrial environments [4]. This research builds upon these foundations, aiming to address the existing gaps in robotics.

III. DESIGN FOR LOW-COST HUMANOID ROBOT ARM

A. Kinematic Modeling and Spatial Analysis

The kinematic configuration of the GRASP-01 is shown in Figure 2, illustrating the joint arrangement and coordinate frames that define the manipulator's motion capabilities with a 7-DOF configuration, allowing for a close human-like range of motion. For acquiring the Denavit-Hartenberg (DH) parameters of the robotic arm, Matlab computational tools were used by importing a Unified Robot Description Format (URDF) file that contained the robot's mechanical architecture in Table I can be seen the resultant DH values obtained. Additionally, a Yoshikawa index test was implemented to test the initial possible range of motion of the robotic arm in a constrained workspace that simulated a range of motion from a human left arm, and its results are shown in Figure 3.

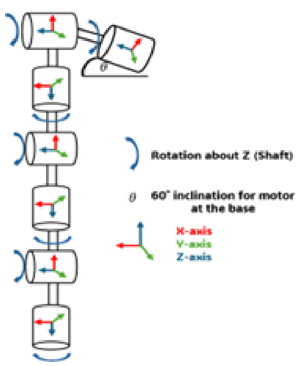

Figure. 2. Kinematic configuration of GRASP-01.

TABLE. I
DENAVIT-HARTENBERG PARAMETERS

Joint	θ (rad)	d (mm)	α (rad)	a (mm)	Offset (rad)
Joint 1	-0.02717	0.15793	2.1817	0.07253	0
Joint 2	1.5415	-0.09	1.5708	0.036484	0
Joint 3	-1.2969	0.0366	-1.5708	0.18352	0
Joint 4	3.0728	-0.05	1.5708	-0.0022861	0
Joint 5	-1.2969	0.0366	1.5708	0.18256	0
Joint 6	-1.5708	-0.02	-3.0358e-17	1.1102e-16	0
Joint 7	-1.6129	0.30609	-1.5708	0.04755	0

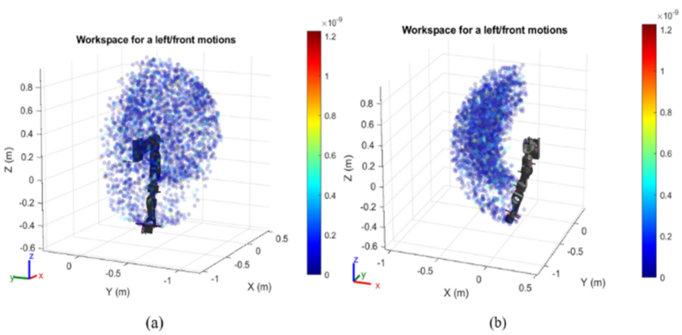

Figure. 3. Yoshikawa Index analysis of GRASP-01.

B. Tensile Test in Polylactic Acid (PLA) Material

The mechanical properties validation of PLA components involved tensile testing of specimens fabricated with identical 3D printing parameters as the robotic arm components in Table III. This methodology ensures accurate material behaviour representation in the FEA simulation. Figure 4 illustrates the Stress-Strain relationship obtained from five test specimens. Although five specimens underwent testing, only three tests (1, 2, and 5) yielded data suitable for comparison with the results reported in [11]. The experimental values differed significantly from the previously documented results. Therefore, material property data from [12] provided more reliable benchmarks for the simulation parameters.

As shown in Table 2, tests 1, 2, and 5 provided valid data for material analysis, while tests 3 and 4 required exclusion due to specimen failure during testing. The notable disparity in Young's Modulus values across specimens highlights the inherent variability in FDM materials such as PLA. The experiment operated at 5 mm/min, with dimensions according to ASTM D638: total length of 165 mm, thickness of 3.2 mm, and gauge length of 50 mm. Material availability constraints for this prototype were limited to PLA, though possible use of different materials with better mechanical properties could be implemented later on the prototype.

TABLE. II
VALIDATED TENSILE TEST RESULTS OF PLA SPECIMENS

Specimens	Young's Modules (MPa)	Poisson's Ratio	Shear Modulus (MPa)
Test 1	1237.8	0.3	476.09
Test 2	3131.2	0.3	1204.3
Test 3	7677.6	0.3	2952.9

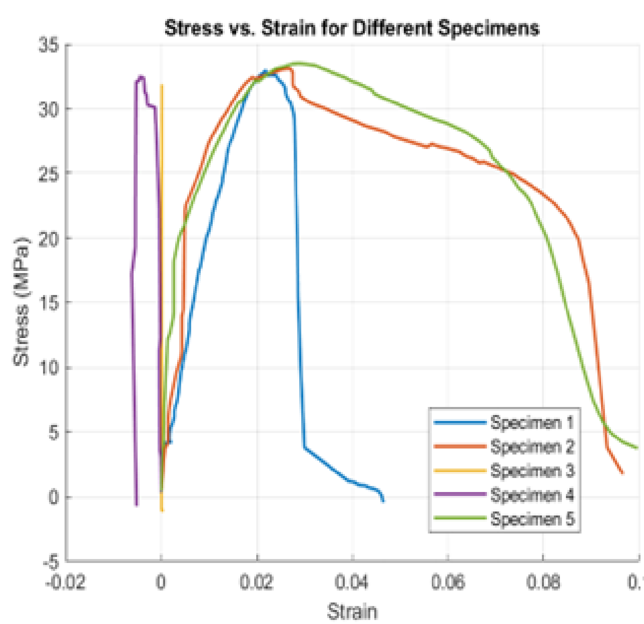

Figure. 4. Stress-Strain curves from tensile testing of PLA specimens.

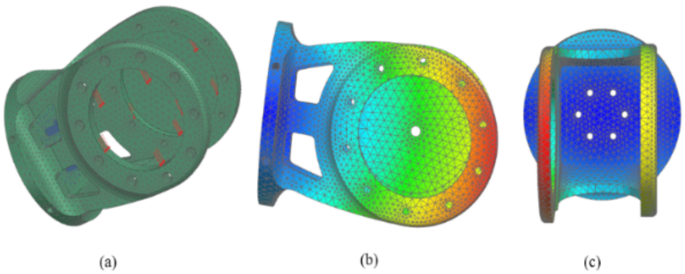

Figure. 5. FEA simulation heatmap results at shoulder component.

TABLE. III
BASELINE PRINT PARAMETERS FOR ALL COMPONENTS

Parameters	Value
Layer Height	0.16 mm
Wall Loops	3
Infill Density	50%
Infill Pattern	Cubic
Initial Layer Speed	50 mm/s
Outer Wall	60 mm/s
Inner Wall Speed	150 mm/s

C. FEA Simulation Results

Finite element analysis (FEA) was conducted on all major joints of the GRASP-01 using established PLA material properties from [12]: Young's Modulus of 3600 MPa, mass density of 0.00000341 kg/mm3, Poisson's ratio of 0.35, and shear modulus of 2400 MPa. The models incorporated mesh generation, geometric constraints based on component interfaces, and force applications accounting for internal, external, and gravitational effects. Thermal mapping analysis identified critical stress points, enabling iterative design optimization. Subsequent physical validation confirmed the structural integrity of the final design; the result can be seen in Figure 5, and the print parameters are listed in Table 3. It shows stress distribution through heat map visualization, where blue indicates low-stress regions and red indicates high-stress concentrations. Critical stress concentrations were identified at the motor mounting interface, suggesting additional structural reinforcement was needed. The analysis identified the central sectioned region as a key area of interest for design optimization.

D. NX Motion Simulation Results

The NX Motion simulation study evaluated dynamic performance under operational loading conditions. Simulations employed a multi-body dynamics approach with precise mechanical properties and full kinematic constraints reflecting the 7-DOF configuration. The analysis provided force and torque values for key joints, which are summarized in Table IV. Results were validated through static force calculations to ensure computational accuracy. These systematic simulations established the maximum torque requirements for proper motor selection and identified critical mechanical stress points.

TABLE. IV
NX MOTION ANALYSIS RESULTS ABSOLUTE AND TORQUE VALUES

Joint Number	**Location**	**Maximum Value**	
Joint 2	Upper/Lower Shoulder	Absolute Force	190 N
Joint 2	Upper/Lower Shoulder	Required Torque	31.9 N/m
Joint 4	Elbow	Absolute Force	160 N
Joint 4	Elbow	Required Torque	31.9 N/m
Joint 7	Wrist	Absolute Force	33.39 N
Joint 7	Wrist	Required Torque	4.19 N/m

IV. SYSTEM INTEGRATION

The GRASP-01 prototype implements a control architecture using Ubuntu 22.04 with CAN bus communication at a 1 Mbps data rate. Initial validation utilized a Python SDK for direct motor control, leveraging the integrated PI controllers for preliminary position control testing. Analysis revealed significant inertial effects at the forearm due to length and payload mass during dynamic movements, necessitating dimensional optimization while maintaining operational requirements. The refined specifications are documented in Table V, with the control framework establishing critical parameters for future iterations. FEA and motion simulation analyses indicate that GRASP-01's design could withstand loads over 2 kg. However, initial testing found 2 kg as the maximum payload capacity at which the current system version maintains stability without exhibiting any oscillations or structural deformations. Unlike the "Blue" robotic arm [6], whose 2 kg payload limitation is due to its timing belt transmission system, GRASP-01's motors offer a direct power transmission with reduced mechanical losses. This payload limit will continue to be used as a conservative operational threshold while development and optimization are needed to achieve higher payload values.

TABLE. V
GRASP-01 CURRENT CONFIGURATION

GRASP-01	Value
Mass	5.6 kg
Reach Full Extension	0.75 m
Reach mid-range	0.375 m
Payload tested	2 kg
DOF	7
Communication	CAN Bus
Control	PI controller

TABLE. VI
GRASP-01 COST BREAKDOWN

Component Type	Cost (CAD)
Motors	4,774.33
PLA Material	107.96
Electronics	139.08
Miscellaneous	148.08
Total	5,169.45

V. COST ANALYSIS

The GRASP-01's development costs are predominantly driven by the high-precision actuator selection, which constitutes the primary cost component. Secondary cost factors include electronic components and miscellaneous hardware required for system integration and assembly. While the system's actuator costs exceed those reported in [6], where quasi-direct drive actuation with timing belt configurations was implemented, the selected integrated servo motors provide greater design flexibility by eliminating the requirement for additional power transmission components. The structural components, fabricated through additive manufacturing using PLA material, represent a significantly lower proportion of the total system cost. As detailed in Table VI, the complete mechanical structure required four PLA filament rolls, demonstrating the cost-effectiveness of additive manufacturing for prototype development. This cost distribution highlights the project's emphasis on high-performance actuation while maintaining economic efficiency in structural component fabrication.

VI. FUTURE WORK)

Several key areas for development have been identified to enhance GRASP-01's capabilities, such as mechanical optimizations, end-effector addition, control system enhancements, sensor integration, and motor controller fine-tuning. Strategic components will be transitioned from PLA to more rigid materials to enhance the structure of GRASP-01. This transition will be part of the mechanical optimizations to reduce high-stress areas. Moreover, the integration of an end-effector will also be contemplated to execute future tests where manipulation of objects will be necessary. While the current version of GRASP-01 is controlled with the integrated position control of the motors, future integration of a robust control system is also in the scope of future work, including more sensors along the arm necessary to integrate different control systems. Finally, the motor controller will be fine-tuned to reduce the possibility of overshooting or unpredictable motions.

VII. SUMMARY

This paper introduced GRASP-01, a 7 DOF humanoid robotic arm leveraging FDM technology to produce a low-cost yet functional design. Achieving a total weight of 5.6 kg distributed along its links, it incorporates compact integrated servo motors that benefit the design by reducing the size of the components and offering position control with CAN bus communication. GRASP-01 achieved a total of 0.75 meters for its reaching capabilities. Testing established 2 kg as the maximum payload capacity without introducing oscillations or deformations in the mechanical components. However, FEA and motion studies suggest the potential for higher load capacity with further enhancements. Using Computer-Aided Design (CAD) software, the design's mechanical robustness was validated using FEA and NX motion simulations to ensure optimal joint performance. While the tensile test performed was not enough to fully validate PLA mechanical parameters, it approximated the values to those found in [11] and [12] to properly set up FEA simulations to get a better understanding of the regions with high stress to optimize them finally. Selecting a modular design throughout the joints could facilitate future enhancements. The project demonstrated positive results in designing and prototyping high-precision components with low-cost materials such as PLA, confirming the potential of scaling robotic development at robotics research labs or education usage.

VIII. ACKNOWLEDGMENTS

The Natural Science and Engineering Research Council of Canada (NSERC) funded this research through the Discovery Grant program (RGPIN-2024-06516).

REFERENCES

[1] Y. Tong, H. Liu, and Z. Zhang, ”Advancements in Humanoid Robots: A Comprehensive Review and Future Prospects,” IEEE/CAA J. Autom. Sinica, vol. 11, no. 2, pp. 301–328, February 2024, doi: 10.1109/JAS.2023.124140. (*references*)

[2] E. Musk, ”According to Elon Musk, this will be the selling price of Tesla's humanoid robots,” CE Noticias Financieras, English ed., Miami, US Minor Outlying Islands, April 10, 2024. [Online]. Available: http://search.proquest.com.uproxy.library.dc-uoit.ca/wire-feeds/according-elon-musk-this-will-be-selling-price/docview/3037280898/se-2?accountid=14694. Accessed: January 19, 2025.

[3] M. Alshihabi, M. Ozkahraman, and M. Y. Kayacan, ”Enhancing the reliability of a robotic arm through light-weighting and vibration control with modal analysis and topology optimization,” Mechanics Based Design of Structures and Machines, pp. 1–25, September 2024, doi:10.1080/15397734.2024.2400207.

[4] S. Mick et al., ”Reachy, a 3D-printed human-like robotic arm as a testbed for human-robot control strategies,” Front. Neurorobot., vol. 13, p. 65, August 2019, doi: 10.3389/fnbot.2019.00065.

[5] F. Hrdlička, ”3D printed planetary gearbox for robotic arm joints,” DMS, vol. 12, no. 1, pp. 38–46, May 2022, doi: 10.32972/dms.2022.004.

[6] D. V. Gealy et al., “Quasi-Direct Drive for Low-Cost Compliant Robotic Manipulation,” in 2019 International Conference on Robotics and Automation (ICRA), Montreal, QC, Canada: IEEE, May 2019, pp. 437–443, doi: 10.1109/ICRA.2019.8794236.

[7] Y. Zhao, B. Huang, S. Lin, Z. Zhu, and Z. Jia, ”A Lightweight Quasi-Direct Drive Collaborative Robot Arm,” in 2023 9th International Conference on Mechatronics and Robotics Engineering (ICMRE), Shenzhen, China: IEEE, Feb. 2023, pp. 24–29. doi: 10.1109/ICMRE56789.2023.10106520.

[8] D. Chowdhury, Y.-E. Park, I. Jung, and S. Lee, ”Characterization of Exterior Parts for 3D-Printed Humanoid Robot Arm with Various Patterns and Thicknesses,” Polymers, vol. 16, no. 7, p. 988, Apr. 2024, doi: 10.3390/polym16070988.

[9] J. Costa, T. Antônio Urzedo Machado, and M. Carneiro, “Implementation and Validation of Thor 3D Printed Open Source Robotic Arm,” IEEE Latin Am. Trans., vol. 18, no. 05, pp. 907–913, May 2020, doi: 10.1109/TLA.2020.9082919.

[10] A. K. Nuhel, M. M. Sazid, Md. N. M. Bhuiyan, and A. I. Arif, ”Designing and Performance-Analysis of a 3 DOF Robotic Manipulator Arm and its Higher Order Integration for 7 DOF Robotic Arm,” in 2022 4th International Conference on Sustainable Technologies for Industry 4.0 (STI), Dhaka, Bangladesh: IEEE, Dec. 2022, pp. 1–6. doi: 10.1109/STI56238.2022.10103352..

[11] C. Grabowik, K. Kalinowski, G. Ćwikła, I. Paprocka, and P. Kogut, ”Tensile tests of specimens made of selected group of the filament materials manufactured with FDM method,” MATEC Web of Conferences, vol. 112, p. 04017, 2017, doi: https://doi.org/10.1051/matecconf/201711204017.

[12] Matweb, ”Overview of Materials for Polylactic Acid (PLA) Biopolymer,” https://www.matweb.com/search/DataSheet.aspx?MatGUID=ab96a4c0655c4018a8785ac4031b9278&ckck=1